Separation Patterns of Boundary Layer over an Inclined Body of Revolution

K. C. WANG*
RIAS, Martin Marietta Corporation, Baltimore, Md.

Based on recent symmetry-plane boundary-layer solutions, new separation patterns over an inclined body of revolution are presented. Support by experimental evidence as well as differences from other predictions in the literature are noted. Existing three-dimensional separation criteria are mostly inapplicable, and the resulting patterns found are compatible only with Maskell's general description of separation—i.e., a combination of the free vortex layer type and a bubble type. For a not too blunt body, a bubble type prevails at low incidence, and a free vortex layer type dominates a high incidence. At extremely high incidence or for a more blunt body, a bubble type prevails again.

Nomenclature

a = semimajor axis
A = regular boundary region
b = semiminor axis
B = embedded vortex region
C = separated region
p = pressure
R = vortex starting point
S = separation point
u = meridional velocity
v = circumferential velocity
w = normal velocity
$\partial v/\partial\theta$ = circumferential derivative of v
z = normal coordinate
α = incidence angle
μ = meridional coordinate
θ = circumferential coordinate

I. Introduction

THIS paper presents a nonmathematical discussion of the separation of the three-dimensional laminar boundary layer over an inclined body of revolution. The main ideas are drawn from the author's recent works on the symmetry-plane boundary-layer solution[1,2] and are supported by limited experimental evidence.[3,4] Some elements of these can be traced to previous investigations,[5-10] such as those of Maskell[6] and Nonweiler.[7] However, the resulting separation patterns differ from earlier proposals and the main theme of argument is based on recent works[1,2] and has not appeared elsewhere.

Section II recapitulates some results from the symmetry-plane solutions for a spheroid which pertain to the separation question. These symmetry-plane results not only specify the flow pattern near the symmetry plane, but they also shed light on the flow over the entire body surface.

In Sec. III a picture of the complete surface flow patterns over a spheroid is proposed. At high incidence, there are at least two stages of separation. A free vortex layer type of separation occurs first, followed downstream by a bubble type of more conventional nature. At low incidence or extremely high incidence there is only a single stage of separation (of the bubble kind), in spite of the fact that the circumferential flow exhibits reverse phenomenon. Decrease of thickness at a fixed incidence causes effects similar to those of increasing incidence for fixed thickness. For a fat spheroid, the separation pattern will always be a bubble type.

Comparisons with experiments and other predictions in the literature are made in Sec. IV. It is seen that our proposed surface flow patterns are supported by the experiment of Stetson and Friberg[3] and to a lesser degree by those of Werle.[8] They differ in basic nature from those given by Eichelbrenner and Oudart,[11] but agree in some aspects with those of Maskell,[6] Nonweiler,[7] and Cooke and Brebner.[10]

The resulting separation patterns are examined in Sec. V to test the applicability of existing theories[6,12-16] on three-dimensional separation. Among these theories, our results are found to be compatible only with Maskell's[6] general description. He suggests that a combination of the bubble and the free vortex layer types of separation is, perhaps, the most likely general form of flow separation. The question of how to determine the separation line in actual numerical calculations is also touched upon.

Finally, in Sec. VI, by drawing an analogy from a number of well-understood examples, such as the supersonic pointed cone and yawed cylinder, one finds that the separation patterns discussed in Sec. III appear to follow as reasonable extensions, and certain common features are characteristic of a whole class of body problems. The fact that these features have not been appreciated is shown by the contradictory versions of the separation pattern which persist in the literature.

Except for Der's work,[17] complete solutions of three-dimensional boundary layers over inclined bodies remain to be presented. However, a better understanding of the physical picture such as presented here can be of great help prior to any attempt at actual computations. Throughout this work, our discussion is confined to the surface flow patterns. Inferences regarding the vortex structure of separated flow have been avoided deliberately.

II. Symmetry Plane Problem

Recently the incompressible laminar boundary layer near the symmetry plane of an inclined prolate spheroid[1,2] was calculated exactly by an implicit finite difference method. The flow configuration is shown in Fig. 1. Two basic quantities which have been determined are the profiles of u and $\partial v/\partial\theta$ (instead of v which vanishes identically) across the boundary layer on both the windside and leeside meridians. Important for our present purpose is the flow condition near the points where $\partial u/\partial z$ or $\partial/\partial z(\partial v/\partial\theta)$

Presented as Paper 71-130 at the AIAA 9th Aerospace Sciences Meeting, New York, January 25–27, 1971; submitted October 15, 1971; revision received March 2, 1972. This research was sponsored in part by the Air Force Office of Scientific Research, Air Force Systems Command, U.S. Air Force, under AFOSR Contract F44620-70-C-0085. The author is indebted to S. H. Maslen for various comments during the course of this work.

Index category: Boundary Layers and Convective Heat Transfer—Laminar.

* Research Scientist. Member AIAA.

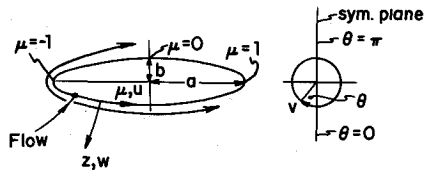

Fig. 1 Flow over a spheroid ($b/a = \frac{1}{4}$).

vanish at the body surface, $z = 0$. The significance of $(\partial u/\partial z)_{z=0} = 0$ at point S (Fig. 2a) is familiar—namely, zero (meridional) skin friction and the onset of the reversal of u-velocity profile. Since $\partial v/\partial z$ is identically zero along the symmetry plane, S is a point at which both components of the skin friction vanish and hence, is a singular point of the limiting streamlines.

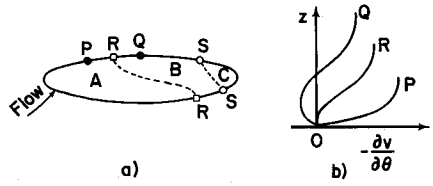

Fig. 2 Reversal of $\partial v/\partial\theta$-profile.

The vanishing of $[\partial/\partial z(\partial v/\partial\theta)]_{z=0}$ at point R (Fig. 2a), signifies the reversal of the $\partial v/\partial\theta$-profile. Since v velocity near but off the symmetry plane varies with μ and z in the same way as $\partial v/\partial\theta$ varies at the symmetry plane, so the reversal of $\partial v/\partial\theta$ profile at the symmetry plane means the reversal of v profile near the symmetry plane. Typical profiles of $\partial v/\partial\theta$ across the boundary layer at three points P, Q, R, on the leeside symmetry plane are illustrated in Fig. 2b. Starting from R, a reversed profile appears. Such reversal may extend as far as halfway across the boundary layer and become more and more pronounced as the incidence increases. In contrast to the point S, R is a regular point of the limiting streamlines because $(\partial u/\partial z)_{z=0}$ does not vanish here. R may be termed[1,2] the vortex starting point and S the separation point.

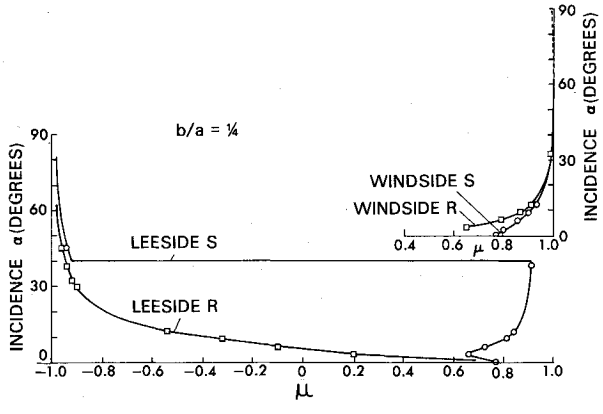

Fig. 3 Variation of points R and S with incidence.

The calculated locations of points R and S vs incidence for a prolate spheroid ($b/a = \frac{1}{4}$) are shown in Fig. 3 (Ref. 2). R is seen to be located ahead of S. On the leeside, as the incidence increases, R continues to move forward. S moves forward first ($0° \sim 3°$) and backward later until the incidence is about 40°; then it jumps to the front. On the windside, both R and S move rearward with increasing incidence, and the distance between them always remains small.

This figure suggests significant departures from the usual separation concepts. The very appearance of R ahead of S contradicts the usual notion that no reversed flow exists before the separation point S. Contrary to the usual expectation that S continuously moves forward with the increase of incidence, it turns out to be R instead which really behaves this way, while S moves forward and backward. It is intuitively expected that at extremely high incidence (say $>45°$ for a spheroid with $b/a = \frac{1}{4}$), S eventually will be located at the front due to an insurmountable adverse pressure gradient there; however, it is not obvious that this change takes place in the form of a sudden jump. Further confusing in this respect is the fact that prior to such jump, S moves rearward. This rearward movement of S has since been confirmed by Wilson's experiment[4] in two different ways. Direct observations were made by ejecting smoke from the rear end into the flow near the surface and observing where the smoke was stopped. Indirectly, his careful measurement of the u velocity profile shows the same tendency to become flattened in the downstream direction as do the calculated results.[1,2] A flattened near-uniform u velocity profile leads to delay in separation.

Accompanying this variation of R and S with incidence, other results such as the skin friction and displacement thickness generally show familiar, well-behaved trends on the windside but reveal a number of unconventional features on the leeside. The details are discussed more thoroughly in Ref. 2.

If we connect points R on the windside and leeside and do the same for the S points, the flow is divided into three regions: the regular boundary-layer region A (see Fig. 2a), the embedded vortex region B and the separated region C. At low incidence (say $\alpha < 6°$), it has been noted[1] that region B remains thin (similar to region A). The boundary-layer concepts can still be justified, and the reversal of v velocity suggests an embedded vortex inside the boundary layer. At high incidence, region B is no longer thin, the flow exhibits unusual features and does not behave strictly as a boundary layer (although formal solutions can be obtained).

III. Surface Flow Patterns

The results obtained previously[1,2] not only specify the limiting streamline pattern near the symmetry plane, but they also help one to visualize the entire surface flow pattern.

Surface Flow Pattern near the Symmetry Plane

The flow pattern in the vicinity of the symmetry plane is specified by the symmetry-plane boundary-layer results[1,2] (Fig. 4).

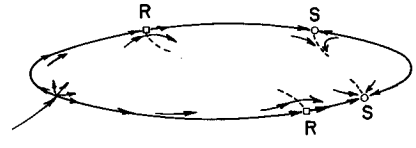

Fig. 4 Surface flow pattern near the symmetry plane.

Near the point R the v velocity close to the body is reversed, but the u velocity direction remains unchanged up to the point S. The limiting streamline ahead of R is, therefore, directed toward the symmetry plane on the leeside while that downstream of R is directed away from the symmetry plane. Beyond the point S, since the u velocity close to the wall is also reversed, the limiting streamline points upstream and, at the same time, away from the symmetry plane on the leeside. The windside pattern is just the reverse of the leeward one (Fig. 4).

Since R is a regular point, there must be only one continuous limiting streamline passing through R. However, at the singular point S, the limiting streamlines may be discontinuous, and more than one limiting streamline may pass there. On the leeside, the point S is a saddle point of separation; but on the windside, it is a nodal point of separation. The front and rear attachment points (see Fig. 5) also are nodal points. Altogether there are three nodal points and one saddle point. The topological law[1,2] that the number of nodal points must exceed the number of saddle points by two is satisfied.

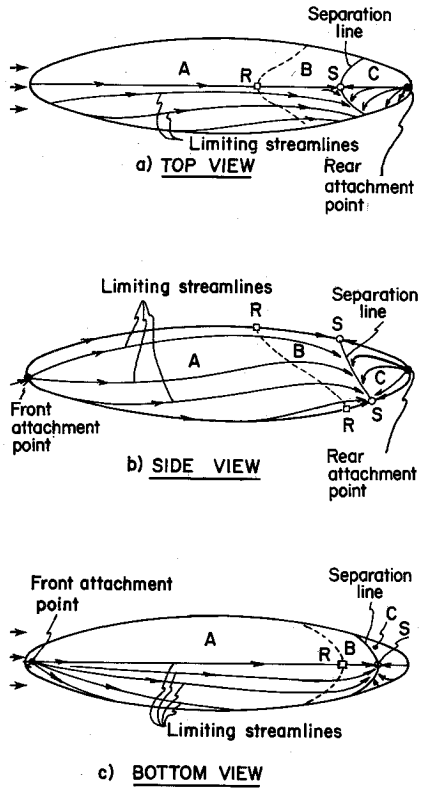

Fig. 5 Surface flow pattern at low incidence (Locations of R and S are based on results for $\alpha = 3°$).

Complete Surface Flow Patterns

Having determined the surface pattern near the symmetry plane from the boundary-layer solutions, one may next postulate the complete surface flow pattern with the aid of experimental evidences and physical intuition. As our discussion moves away from the symmetry plane, we choose to continue to refer to the flow velocity by its components u and v along the meridional and circumferential directions.

As indicated before, the curves RR and SS are hypothesized to divide the surface flow into three distinct regions, A, B and C. To be specific, we define the curve RR to mark the reversal of v velocity or to be the zero circumferential skin-friction line. As far as the surface flow is concerned, region B is characterized by the reversal of v velocity compared to region A. The curve SS is a separation line; its determination will be described later. Region C is a separated region in the usual sense. The surface flow patterns in regions A and C are easier to visualize with the usual boundary-layer concepts. But the pattern in region B is different; it may take different forms with different physical significances, depending on the incidence and geometry. It is the surface flow in this region which differs from what has been presented in the literature.

It is understood that, for a surface flow, the choice of a coordinate system is arbitrary. The curve RR and the region B just defined are related to the v velocity of the geodesic coordinates used. This serves our purpose to describe the physical flow phenomena adequately even if not most precisely.

Low-incidence case

Our symmetry-plane results[1,2] indicate that at low incidence (say 3°), R and S are close together on both the windside and the leeside so that region B is fairly narrow. Despite a small portion near the wall exhibiting reversal of v velocity, the boundary layer there otherwise behaves well in all aspects, including the u velocity profile, skin-friction distribution and very thin boundary-layer thickness. The partially reversed (i.e., v velocity only) flow under such circumstances may be considered as a sort of vortex embedded inside the boundary layer.

On this basis, region B is not considered as "separated" in spite of the occurrence of reversed flow. As each limiting streamline crosses the curve RR (Fig. 5), it reverses its v velocity direction. Being at low incidence, the meridional flow is dominant over the circumferential part. Although it may be adverse over the leeside surface, the circumferential pressure gradient is small; the limiting streamlines are therefore expected to cross the curve RR smoothly without being forced to run along the curve RR. Farther downstream, all the limiting streamlines are diverted to follow the separation line SS. This type of separation is not much different from that of the familiar axisymmetrical case and may be classified as the bubble type (see Sec. V). The separation line SS passes through the singular points on the symmetry plane and divides the flow originating from the front attachment point from that originating from the rear attachment point.

High-incidence case

The symmetry-plane solutions[1,2] revealed that at high incidence (say $\alpha > 12°$ for a spheroid with $b/a = \frac{1}{4}$), points R and S on the leeside are far apart, and region B covers most of the leeside of the body surface. Region A continues to exhibit familiar boundary-layer behavior. However, unlike the low incidence case, the flow in region B now behaves far differently from a typical boundary layer.† The unusual features include, for example, the strongly reversed v velocity profiles and the extremely large boundary-layer thickness. These suggest that some sort of separation must have taken place. Since only the v velocity reverses its direction, but not u velocity, the suspected separation must be essentially a kind of circumferential flow separation. Also, since the limiting streamlines near the symmetry plane can still penetrate from region A to region B, the separation line (really a curve) must be open at both ends, i.e., it does not extend to intersect the symmetry plane.

These considerations lead to the idea of the separation line I sketched in Fig. 6 to signify the first stage of separation. A procedure of determining this line during the numerical computation

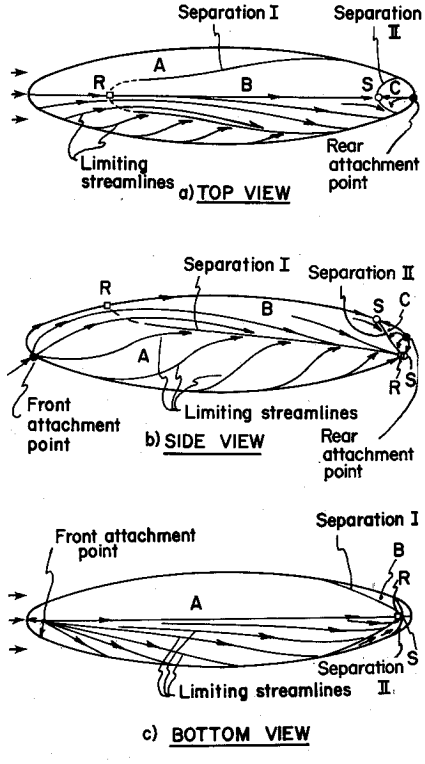

Fig. 6 Surface flow pattern at high incidence (Locations of R and S are based on results for $\alpha = 12°$).

† The state of the leeside flow is discussed in Ref. 2. The symmetry plane solutions obtained check well in basic trends with experiments,[3,4] but little is described there for the complete leeside problem away from the symmetry plane.

is discussed later in Sec. V. Roughly the separation line I should run closely to the curve RR but not necessarily coincide with it. This line is characterized by its approach from two sides by two different sets of limiting streamlines; both sets originate from the same front attachment point. Such a structure appears to be of the free vortex layer type discussed by Maskell[6] (see Sec. V), although this identification is solely based on the limiting streamline pattern at the present time. What appears to happen here is that before reaching the separation line I from the windside, the flow under strong circumferential adverse pressure gradient loses much of its momentum and hence cannot penetrate too far before being diverted. Since the separation line I and the curve RR are believed to be close to each other, the region B bordered by the curve RR is nearly the same as the separated region bordered by the separation line I. To avoid introducing additional labels, we shall make no distinction between them in later discussion. Note that in Fig. 6 only a portion (near the symmetry plane) of the curve RR is actually shown by the broken line.

Farther downstream, the flow is again diverted to follow the separation line SS, which is redesignated in Fig. 6 as the separation line II to signify the second stage of separation. The surface flow in region C here is basically the same as the region C of Fig. 5 for the low-incidence case.

Although region B at high incidence is also a kind of separation region, there are obvious differences in the surface flow between these regions B and C. Region B exhibits reversal of v velocity; region C exhibits the reversal of both u and v velocity. The term "reversal" again is meant with respect to the corresponding velocity component in the regular region A. The flow in region B originates from the front attachment point, while flow in region C originates from the rear attachment point. Also region C is a closed region, but region B is an open one (because the separation line I is not closed).

It should be pointed out that the flow pattern in region B can be more complicated than indicated in Fig. 6. There may be reattachment and secondary separation (see, for examples, Fig. 12), although such phenomena are not well understood. It is safe to say that there are, at least, the two separation lines, I and II shown in Fig. 6.

Extremely high incidence

As the incidence continues to increase (say $\alpha > 40°$ for a spheroid with $b/a = \frac{1}{4}$), the symmetry-plane solutions show that both points R and S on the leeside are located at the front, and region B nearly disappears. The separation reverts to a closed bubble type (Fig. 7), and the separation line SS is aligned more closely with the meridians rather than with the parallels, as in Fig. 5 for low incidences.

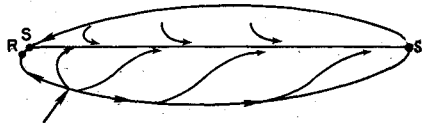

Fig. 7 Surface flow pattern at extremely high incidence (Locations of R and S are based on results for $\alpha = 45°$).

Thickness effect

The foregoing discussion is based on the results for a fixed moderate thickness ratio ($b/a = \frac{1}{4}$) at various incidences. These separation patterns naturally will change with the body thickness. The effect of a change in thickness on the separation is shown in Fig. 8, which gives the location of points R and S at a fixed incidence ($\alpha = 12°$) for a spheroid with different thickness ratios.

On the windside, R and S are always very close to each other and move rearward with decreasing thickness. On the leeside, the situation is different. As the thickness decreases, S moves forward and then backward, while R continues to move forward. The boundary layer for $b/a = 0.125$ at 12° incidence exhibits many of the same characteristics as the boundary layer for $b/a = 0.25$ at

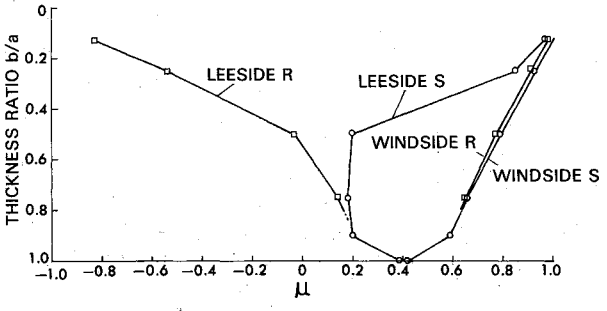

Fig. 8 Variation of points R and S with thickness.

nearly 30° incidence. In other words, a more slender body is more sensitive to the incidence effect. The previously described cycle, namely bubble-free vortex layer-bubble, holds also for more slender bodies, except that the changes occur at lower incidence. For example, the change from the free vortex layer type to the bubble type for a spheroid of $b/a = 0.125$ is likely to occur at an incidence of 20° instead of 40° for a spheroid of b/a equal to 0.25. On the other hand, for a fatter spheroid, R and S are so close that the separation pattern will be always a bubble type.

IV. Comparisons With Experiments and Literature

In this section we shall cite some experimental evidence relating to the separation patterns just proposed. We shall also compare our version with others already known in the literature and point out the agreements and the differences.

Experimental visualizations of the surface flow pattern over bodies of revolution at incidence have been conducted by a number of investigators.[3,8,9] Results for pointed bodies (mostly circular cones) are consistent and conclusive, but for blunt bodies, the photographs often are not clear enough to indicate a well-defined separation line. This situation contributes to some misconceptions and confusion surrounding the subject.

Experiment by Stetson and Friberg[3]

Figure 9 shows the separation pattern of a hypersonic blunt cone at an incidence of 10° due to Stetson and Friberg. The separation line is clearly visible. Note that two oil streaks proceed from the nose region right through the separated region, demonstrating that the separation region is not closed in the front.

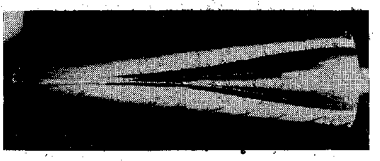

Fig. 9 Blunt cone at incidence, top view (from Stetson and Friberg).

This experimental picture agrees with our Figs. 4 and 6. Stetson and Friberg's separated region may be identified as the region B; their converging-diverging flow pattern agrees with that pictured near R in Figs. 4 and 6. Being a cone, obviously there is nothing like point S far downstream on the leeside or points R and S on the windside. Since the experiment of Stetson and Friberg was for hypersonic flow, while our present discussion is exclusively for incompressible flow, one might question the validity of using their results to support our argument. However, it is believed that, particularly for a simple shape like a blunt cone, the basic features of the surface flow should be qualititatively the same in high as in low-speed flow.

Werle's Separation Patterns

Werle[8] studied the separation patterns over a number of bodies of revolution. Relevant to our concern here is his more slender (front-half) configuration reproduced here in Fig. 10 which he sketched from an experimental photograph.

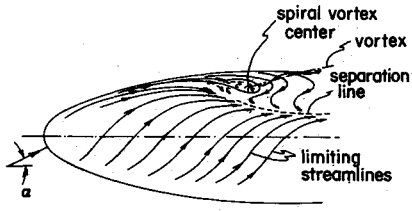

Fig. 10 Werle's separation pattern over a blunted body at high incidence (side view, $\alpha = 20°$).

Apart from the strange pair of spiral vortices, Fig. 10 suggests some important features similar to those in our sketches, Fig. 6. Specifically, 1) the limiting streamlines near the leeside symmetry plane run straight into the separated region, and the separation line is open in the front end, and 2) the separation is basically a circumferential-flow separation.

Werle[8] also investigated the surface flow patterns over more blunted bodies at high incidence ($20° \sim 30°$). The resulting patterns appear to be of the bubble type and hence are in agreement with our conclusion about the thickness effects. But his pictures showing complicated vortices inside the separation region are difficult to interpret.

Eichelbrenner's and Oudart's Separation Pattern

Figure 11a shows the separation picture (top view) for a prolate spheroid ($b/a = \frac{1}{6}$) at an incidence of 10°. This picture is reproduced from Schlichting's book,[18] and was originally due to Eichelbrenner and Oudart.[11] However we believe that this picture is incorrect. To support this claim, we calculated the symmetry plane boundary layer for this specific case (i.e., $\alpha = 10°$ and $b/a = \frac{1}{6}$). Our results show that points R and S are located at μ equal to -0.625 and 0.940 on the leeside, and these points on the windside are at 0.940 and ~ 1.0. Their point S on the leeside is roughly at the mid-station ($\mu = 0$); ours in near the rear end.

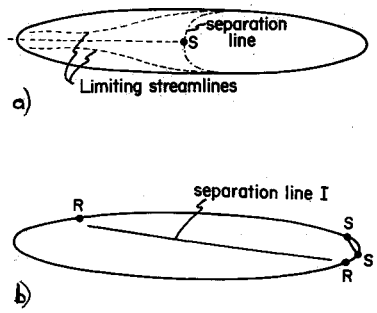

Fig. 11 Separation pattern over an inclined spheroid $b/a = \frac{1}{6}$, $\alpha = 10°$: a) Top view due to Eichelbrenner and Oudart; and b) Proposed side view (R and S are based on our symmetry-plane solution).

Similar to Fig. 6, we believe that the separation should appear as sketched in Fig. 11b. While their pattern belongs to a bubble type, ours is mainly a free vortex layer type.

Nonweiler's Flow Patterns

Figures 12a, b reproduce Nonweiler's[7] view of the surface flow patterns over a body of revolution. Figure 12a, for low incidence, is based on his circumferential boundary-layer analysis. Figure 12b, for higher incidence (Nonweiler termed it moderate), is based on experiment as well as physical intuition.

Comparing Fig. 12a with the rear part of Fig. 5, one finds that in both cases the limiting streamlines (which Nonweiler called "surface streamlines") are curved downward (side view) due to the reversal of v velocity. However, separation due to the longitudinal reversal is missing from Fig. 12a; such separation would generally occur even in a zero incidence case.

From the side view of Fig. 12b (where the label "separation line I" was inserted by this author), one can readily identify a separation line I similar to that shown in Fig. 6. Its structure seems to be also of Maskell's free vortex layer type. However,

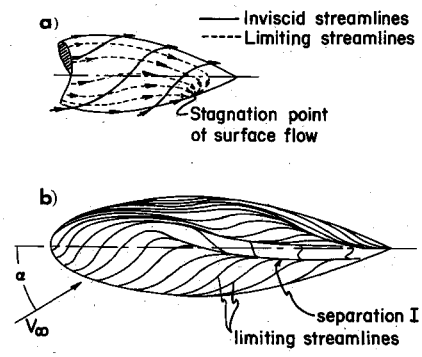

Fig. 12 Nonweiler's surface flow patterns (from Thwaites): a) low incidence; and b) moderate incidence, $\alpha = 20°$.

Fig. 12b gives no indication about the separation line II relating to a bubble type of separation. On the other hand, Nonweiler's more detailed picture showing reattachment and secondary separation has not been taken into account in our sketches, because little is really well understood along that line.

Cooke's and Brebner's Patterns

Figures 13a, b give the flow patterns sketched by Cooke and Brebner[10] respectively for incidence larger and smaller than 9°. Since their geometry is also a prolate spheroid, comparison is more appropriate. The thickness ratio in their sketches is roughly $\frac{1}{2}$ and so is fatter than that considered in Figs. 5 and 6. As noted before, for a fatter spheroid, the points R and S move close, and the separation is always of a bubble type. Therefore we essentially agree with their sketch, Fig. 13a.

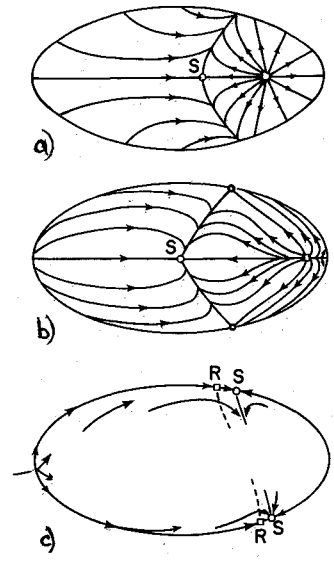

Fig. 13 Separation pattern over a spheroid; a) top view $\alpha > 9°$, b) top view $\alpha < 9°$ (Ref. 10) and c) calculated side view near the symmetry-plane for $b/a = \frac{1}{2}$, $\alpha = 6°$.

However, their sketch, Fig. 13b, for incidence less than 9° displays certain opposite trends. As a check to this behavior, we calculated the symmetry plane boundary layer for a spheroid of b/a equal to $\frac{1}{2}$ at an incidence of 6°. The point S is found to be located at μ equal to 0.6808 on the windside and 0.3705 on the leeside. The corresponding locations for R are 0.6351 and 0.2240. The pattern thus obtained near the symmetry plane (Fig. 13c) does not agree with the trend of Fig. 13b; the leeside point S, for example, is still a saddle point as in Fig. 13a rather than a nodal point as in Fig. 13b. Hence, we believe that the pattern of Fig. 13b is not real.

In conclusion, our proposed separation patterns of Sec. III agree with the experiments of Stetson and Friberg and, to a less

extent, with Werle's experiment. Comparison with other predictions known in the literature shows that our surface flow patterns differ in basic nature from Eichelbrenner's and Oudart's but agree in some aspects with those of Nonweiler and Cooke and Brebner. Further comparison with Maskell's patterns will be given in the next section.

V. Separation Criteria

Maskell's Description of Separation

We would like to ask now how the separation pattern presented in Sec. III fits the existing theories[6,12-16] of three-dimensional separation. Eichelbrenner and Oudart first proposed, as the criterion of separation in three dimensions, the condition that the line of separation be an envelope of the limiting streamlines. Maskell[6] pursued this line further and classified the flow involving separation into two basic types—a bubble (Fig. 14a) and a free vortex layer (Fig. 14b). These figures are taken directly from Rosenhead's "Laminar Boundary Layers," although they appeared in slightly different forms in Maskell's original work.[6] Each is characterized by a different form of surface flow pattern. The bubble type requires the existence of a singular point (S in Fig. 14a), while the separation line for a free vortex layer (line LL in Fig. 14b) has only regular points. Maskell remarked that a combination of these two types is, perhaps, the most likely general result of flow separation.

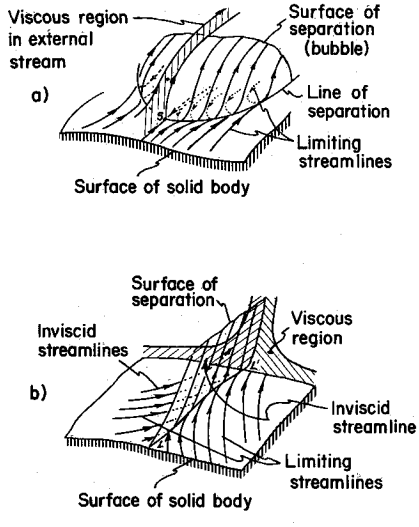

Fig. 14 Maskell's separation concepts. a) Bubble, b) Free vortex layer.

Maskell sketched a number of possible surface flow patterns that might arise on a body of revolution at incidence. Some are of the bubble type, some of the free vortex type, and some are both. Despite certain partial resemblances, his pictures do not contain all the elements we have emphasized in Figs. 5–7. Maskell was not specific in his general treatment; for example, he did not distinguish at what incidence a certain particular pattern may occur. Nevertheless, with the separation line I identified with a free vortex layer type and the separation line II with a bubble type, our surface flow patterns of Fig. 6 represent a way of combining these two and hence are consistent with Maskell's general concept. On both sides of the separation line I (Fig. 6), the limiting streamlines originate from the same front attachment point. This is not what is depicted in Fig. 14b. Our identification of the separation I as the free vortex layer type is therefore not entirely as Maskell originally conceived.

Lighthill's Criterion

In Lighthill's discussion[12] of three-dimensional separation, he defined the line of separation as "a skin-friction line which issues from both sides of a saddle point of separation and, after embracing the body, disappears into a nodal point of separation."

Following this definition, the separation line must be a closed curve on the body surface and must originate from and terminate at singular points. The separation line I of Fig. 6 obviously is ruled out by this definition, since neither of these conditions are satisfied. Hence we must conclude that Lighthill's criterion does not apply to such situations.

Lighthill further stresses that the separation line is itself a limiting streamline. He disputed the idea that the separation line is an envelope of the limiting streamlines. If the separation line is also a limiting streamline, then there must be some special feature which distinguishes this particular limiting streamline from others. In Lighthill's theory, this special feature is that it passes through the singular points. When singular points are not present, as in the case of a blunt cone,[3] the separation line will not be uniquely defined. On the other hand, the envelope concept may still apply. Brown and Stewartson[13] discussed this disputed point at some length; they are in favor of the envelope version. Recent results of Lewis[14] for a symmetrically-disposed ellipsoid also indicate the separation pattern to be of an envelope type. Otherwise this dispute remains to be clarified. Surface visualization experiments usually are not clear enough to distinguish the two.

Actually, the dispute between an envelope and a limiting streamline concept is secondary to whether the separation must even pass through singular points. The latter can have a much greater effect on the final separation pattern.

Other Separation Criteria

There are also separation criteria due to Moore,[15] Hayes,[16] and Stewartson.[13] Moore identified the separation "by the existence of a bubble of fluid in the boundary, not exchanging fluid with its surroundings." One of Hayes' suggestions is to define the separation line as "a particular streamline which separates streamlines coming from an unseparated part of the surface from those coming from a clearly separated part of the surface." Stewartson[13] similarly defined the separation line as "a curve on the body dividing those points that are accessible to the streamline entering the zone of attachment from those points that are inaccessible from attachment."

These three criteria have a common element, i.e., the flows of the separated and unseparated region originate from two different sources. Although this common element is true for the low incidence case shown in Fig. 5, it is not satisfied for the high incidence case shown in Fig. 6 where the flow on both sides of the separation line I originates from a common source.

To sum up, at low incidence and extremely high incidence, the separation patterns are of conventional nature, and all of the aforementioned existing separation theories are by and large applicable. At intermediate incidence, the proposed separation pattern (Fig. 6) is consistent only with Maskell's general description of separation.

Determination of the Separation Line

There still remains an important question: how to determine the separation line. Ideally one would like to have a precise, easy-to-apply mathematical criterion. In the two-dimensional case, this is given by the vanishing of skin friction, $(\partial u/\partial z)_{z=0}$. In the three-dimensional case, there are two components of skin friction; the separation is not determined by the vanishing of either or both of these two components, except in special cases.

In actual computation, it seems, however, that the separation line may be identified by examining the limiting streamline pattern calculated from the results as the computation proceeds. Whenever the limiting streamlines tend to approach a particular line, then this particular line will be taken as the separation line. One may loosely refer to the separation line so obtained as an envelope of the limiting streamlines, but whether this term "envelope" applies in the strict mathematical sense requires further proof.

VI. Further Considerations

We would like now to explore further the separation phenomena for inclined bodies of revolution. By comparing some special, well-understood examples, we wish to show that certain common features become self-evident and that the separation pattern sketched in Fig. 6 appears to follow very naturally. In so doing, one would also see how our foregoing discussions, primarily for a spheroid, also can be carried over to other bodies. Since the separation pattern is controlled by the surface pressure gradients, we shall start from the case for which one component of the surface pressure gradients vanishes, follow by relaxing this restriction over the front end of the body, and finally impose no restriction. For convenience of discussion, we follow the usual convention to denote the surface coordinates x, y and velocities u, v as shown in Fig. 15.

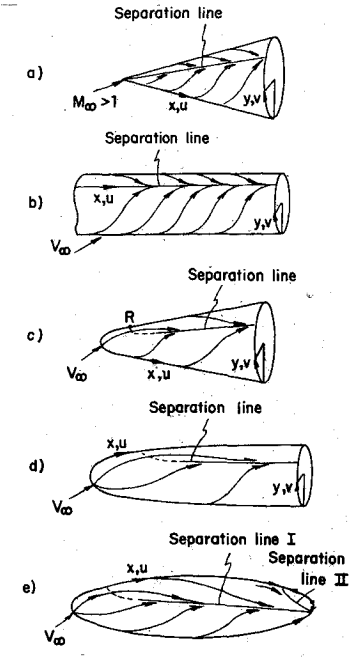

Fig. 15 Separation over inclined bodies.

Case 1, $\partial p/\partial x = 0$: A well-known example of this case is the slender pointed circular cone (Fig. 15a) at incidence in supersonic flow. Here conical similarity solutions for the boundary layer hold. The pressure gradient $\partial p/\partial x$ vanishes identically, but $\partial p/\partial y$ is favorable on the windside and adverse on the leeside. The flow is known to separate along a generator due entirely to the reversal of v velocity near the body, and the separation line is determined by $(\partial v/\partial z)_{z=0} = 0$. Along this separation line, $(\partial u/\partial z)_{z=0}$ is nonvanishing.

When the flow is subsonic or incompressible, we expect that the separation pattern will be much like this and the criterion $(\partial v/\partial z)_{z=0}$ will still hold, even though the flow is not quite conical.

To avoid reliance on the supersonic flow phenomena, it is, perhaps, more appropriate to consider the case of a long cylinder at incidence (Fig. 15b). Again $\partial p/\partial x = 0$ and separation occurs along a generator determined entirely by reversal of v velocity near the body.

Case 2, $\partial p/\partial x \neq 0$ at the front: This case is somewhat less restrictive and occurs in the use of a blunt cone (Fig. 15c) or a blunt cylinder (Fig. 15d). An adverse longitudinal pressure gradient, may exist on the leeside of the front end, but it is usually not large enough to cause the reversal of u velocity near the body. If reversal of u velocity does not occur over the front part of the body, it will never do so, because the flow will behave more and more like that over a pointed cone or an infinite cylinder. The separation is, therefore, still essentially due to the reversal of v velocity or the circumferential adverse pressure gradient. The separation line does not start from the apex; instead, it starts somewhere downstream not earlier than the station R (see Fig. 6). This separation line separates the limiting streamlines originating from the same attachment point.

Case 3, $\partial p/\partial x \neq 0$: This is the general case of a finite body curved on both ends (Fig. 15e). The prolate spheriod discussed before serves as a typical example. Over the front part of the body, one would expect that the flow will be similar to that over a blunt cone (or cylinder); i.e., there is a separation line (designated as the separation line *I*) of the nature described in Case 2. Differences arise only over the rear part of the body, where a strongly adverse longitudinal pressure gradient leads to the reversal of u velocity. The net result is a second stage of separation marked by the separation line *II*. Limiting streamlines inside this latter separated region originate from the rear attachment point.

Throughout these examples, in Cases 1–3 some common features of separation are noteworthy: a) the separation is mainly due to the separation of circumferential flow (i.e., v velocity reversal), b) the separation line does not necessarily originate or terminate at singular points, and c) the limiting streamlines of the unseparated and the separated regions may originate from the same source. These features are physically natural and characteristic of the type of problem concerned, but they have not been explicitly stated as such and clearly appreciated before.

References

[1] Wang, K. C., "Three-Dimensional Boundary Layer Near the Plane of Symmetry of a Spheriod at Incidence," *Journal of Fluid Mechanics*, Vol. 43, Pt. 1, Aug. 1970, pp. 187–209.

[2] Wang, K. C., "Further Investigation of Three-Dimensional Boundary Layer Near the Symmetry Plane of an Inclined Body of Revolution," TR 71-14c, Sept. 1971, RIAS, Martin Marietta Corp., Baltimore, Md.

[3] Stetson, K. F. and Friberg, E. G., "Surface Conditions in the Leeward Region of a Blunt Cone at Angle of Attack in Hypersonic Flow," ARL-69-0014, July 1969, Wright-Patterson Air Force Base, Ohio.

[4] Wilson, G. R., "Experimental Study of a Laminar Boundary Layer on a Body of Revolution," Master thesis GAM/AE/71-4, March 1971, Air Force Inst. of Technology, Wright-Patterson Air Force Base, Ohio.

[5] Allen, H. J. and Perkins, E. Q., "A Study of Effects of Viscosity on Flow over Slender Inclined Bodies of Revolution," TR 1048, 1951, NACA.

[6] Maskell, E. C., "Flow Separation in Three Dimensions," RAE Rept. Aero 2565, Nov. 1955, Royal Aircraft Establishment, Bedford, England.

[7] Nonweiler, T., *Incompressible Aerodynamics*, edited by B. Thwaites, Oxford University Press, Oxford, England, 1960.

[8] Werle, H., "Separation on Axisymmetrical Bodies at Low Speed," *La Recherche Aeronautique*, No. 90, Sept.–Oct. 1962.

[9] Rainbird, W. J., etc., "Some Examples of Separation in Three-Dimensional Flows," *NAE Quarterly Bulletin*, Vol. 1, No. 1966, 1966, Ottawa, Canada.

[10] Cooke, J. C. and Brebner, G. G., "The Nature of Separation and Its Prevention by Geometric Design in a Wholly Subsonic Flow," *Boundary Layer and Flow Control*, Vol. 2, edited by G. V. Lachman, Pergamon Press, New York, 1961.

[11] Eichelbrenner, E. A. and Oudart, A., "Methode de Calcul de la Couche Limite Tridimensionnelle. Application a un Corps Fusele Incline sur le Vent," ONERA Publication 76, 1955, Paris, France.

[12] Lighthill, M. J., *Laminar Boundary Layers*, edited by L. Rosenhead, Oxford University Press, Oxford, England, 1963.

[13] Brown, S. N. and Stewartson, K., "Laminar Separation," *Annual Review of Fluid Mechanics*, Vol. I, Annual Reviews Inc., Palo Alto, 1969.

[14] Lewis, E., private communication, April 1970, Univ. of Western Ontario, London, Canada.

[15] Moore, F. K., "Three-Dimensional Boundary Layer Theory," *Advances in Applied Mechanics*, Vol. IV, Academic Press, New York, 1956.

[16] Hayes, W. D., "The Three-Dimensional Boundary Layer," NAVORD Rept. 1313, May 1951, Naval Ordnance Research Lab., China Lake, Calif.

[17] Der, J. Jr., "A Study of General Three-Dimensional Boundary-Layer Problems by an Exact Numerical Method," *AIAA Journal*, Vol. 9, No. 7, July 1971, pp. 1294–1302.

[18] Schlichting, H., *Boundary Layer Theory*, 4th ed., McGraw-Hill, New York, 1960.